RSC Advances

This article can be cited before page numbers have been issued, to do this please use: X. sheng, Y. Zhou, Y. Yang, Y. Zhang, Z. Zhang, S. Zhou, X. Fu and S. Zhao, *RSC Adv.*, 2014, DOI: 10.1039/C4RA03531C.

ROYAL SOCIETY OF CHEMISTRY

www.rsc.org/advances

View Article Online
DOI: 10.1039/C4RA03531C

Graphical Abstract

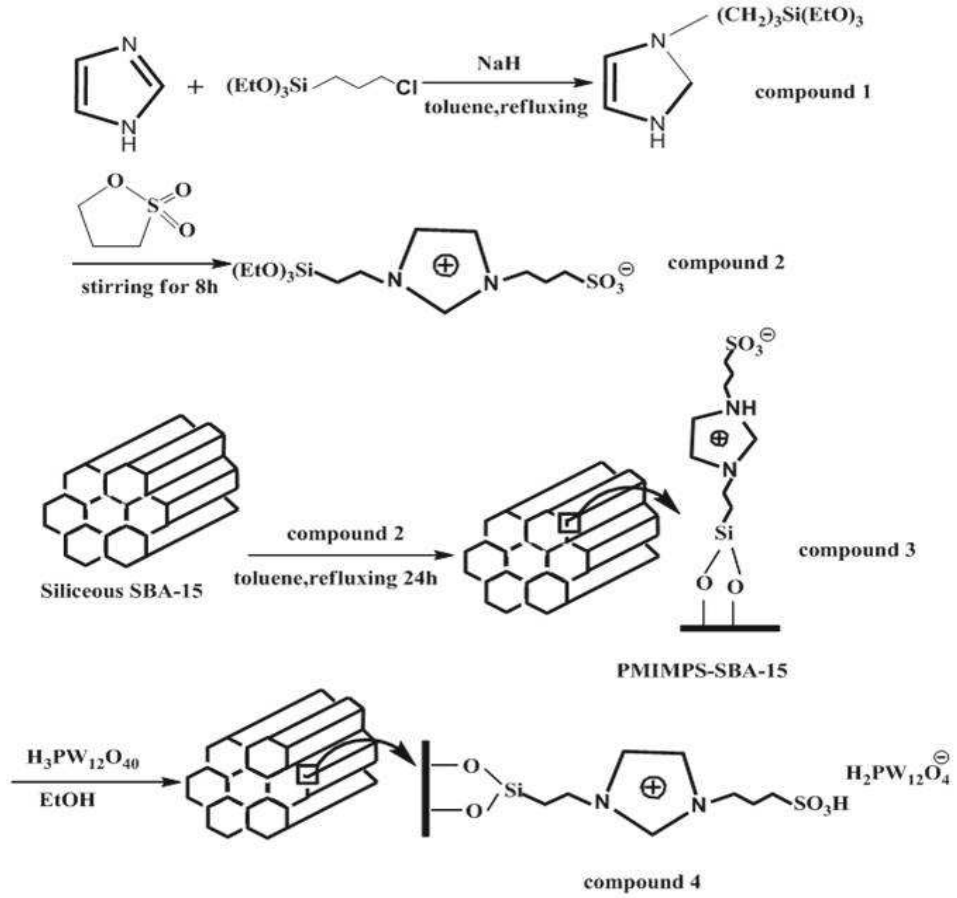

Phosphotungstic acid ($H_3PW_{12}O_{40}$) has been successfully loaded onto sulfonate-functionalized ionic liquid modified mesoporous silica SBA-15 by totally anion-exchange. The obtained catalysts were highly effective for alkylation of *o*-xylene with styrene in terms of yield and stability. Compared with the corresponding pure ionic liquid, both the catalytic stability and reusability were greatly enhanced.

View Article Online
DOI: 10.1039/C4RA03531C

Synthesis of immobilized heteropolyanion-based ionic liquids on mesoporous silica SBA-15 as heterogeneous catalyst for alkylation

Xiaoli Sheng [a], Yuming Zhou [a,*], Yongle Yang [a], Yiwei Zhang [a], Zewu Zhang [a], Shijian Zhou [a], Xiaoqin Fu [a], Shuo Zhao [a]

[a] *School of Chemistry and Chemical Engineering, Southeast University, Nanjing 211189, P.R.China*

Abstract Phosphotungstic acid ($H_3PW_{12}O_{40}$) has been successfully loaded onto sulfonate-functionalized ionic liquid modified mesoporous silica SBA-15 by totally anion-exchange. The immobilized catalysts were characterized by XRD, N_2 adsorption, TEM, and FTIR spectroscopy. Characterization results show that the mesopore structure of SBA-15 was maintained well even after the surface modification and the subsequent anion-exchange step of $[PW_{12}O_{40}]^{3-}$ (PW). In comparison with the task-specific basic ionic liquid (1-(propyl-3-sulfonate) 3-methyl-imidazolium phosphotungstate), the obtained catalyst showed much higher efficiency in alkylation of o-xylene with styrene. More importantly, such immobilized task-specific basic ionic liquid could be reused without significant loss of catalytic activity after 6 times recycling.

*To whom correspondence should be addressed. Tel: +8625-52090617. Fax: +8625-52090617.
E-mail address: ymzhou@seu.edu.cn (Y. Zhou)

View Article Online
DOI: 10.1039/C4RA03531C

1. Introduction

The alkylation of *o*-xylene with styrene to give 1-phenyl-l-arylethane is an industrially important reaction [1]. Phenylxylylethane(PXE) is a colorless synthetic liquid with many excellent properties suitable for various applications, e.g., solvent for pressure-sensitive record materials, plasticizer, heating medium, electric-insulating oil and high-boiling solvent [1]. Nevertheless, one of the main problems in this reaction is the formation of styrene oligomers generated as byproducts, especially when homogeneous Brønsted or Lewis acid catalysts (such as H_2SO_4, BF_3, HF, $AlCl_3$ or $FeCl_3$) are used [1]. Such the aforementioned traditional acids are generally related to problems of high corrosiveness, poor shape-selectivity, low hydrothermal stability and difficulties in waste acid treatment. The hastily demand for environmentally friendly catalytic technology urges development of heterogeneous catalysts thanks to their advantages such as high activity and selectivity, ease of separation and reusability. For PXE synthesis, a monumental series of solid acid catalysts such as silica-alumina [2], cation-exchange resins [3], sulfated zirconia/titania [4, 5], heteropolyacid salts [6] and modified mesoporous silicas [7, 8] are adopted as catalysts, all of which have promoted the catalytic activity. However, these catalysts have disadvantages as well, for example, the compatibility of reusability, operation loss, and high mass transfer resistance, which limit their practical application in alkylation.

Among the recent developments in catalysis, ionic liquids(ILs) have been attracted much attention as being environmental-friendly reaction media for their unique properties of high thermal stability, negligible vapor pressure, tunable acidity and selective dissolvability [9, 10]. Though ionic liquids possessed such promising advantages, their widespread practical application was still hampered by several drawbacks such as unendurable viscosity, high cost, tedious purification procedure of the product and requirements of long reaction time [11]. Therefore, in order to overcome the above shortcomings, immobilized ionic liquid catalyst combining the advantageous characteristics of ionic liquids, inorganic acids and solid acids had been proposed [12, 13].

Indeed, rapidly increased reports have become available describing the use of the ILs immobilized on various supports in the Friedel-Crafts reactions [14]. Ho¨ lderich et al. [15] developed a process for the alkylation of benzene, toluene, naphthalene, and phenol with dodecene in the presence of immobilized 1-butyl-3-methyl-imidazolium chloride with $AlCl_3$ (Al-IIL). The immobilized IL played an important role in significant reduction of overall cost of the process. A

View Article Online
DOI: 10.1039/C4RA03531C

comparison of different supports showed that carriers based on SiO_2 and Al_2O_3 retained higher amounts of chloroaluminate IL than ZrO_2 and TiO_2 carriers after the extraction, and only the silica-based supports were active in the alkylation reactions. In 2009, Yin and co-workers [16] reported the preparation and catalytic activity of novel periodic mesoporous organosilica (PMO) materials incorporating Lewis acidic chloroindate(III) ionic liquid moieties. It was observed that the immobilization of the Lewis acidic ionic liquids with increasing amount of $InCl_3$ led to a drastic increase in the catalytic activity ranging from 14 to 100 conversions with constant selectivity of 100%.

It is well known that Lewis acidic chloroindate(III) ionic liquid moieties is limited to anions with a high affinity to oxygen. Therefore, Brønsted acidic ILs used in some acid-catalyzed processes have aroused considerable interest since they show higher stability towards air and water [17]. With those points in mind, we designed a new heteropolyanion-based ILs containing the sulfonic acid functional group as "task-specific" catalysts immobilized on mesoporous silica SBA-15. The immobilized catalysts were fully characterized by XRD, N_2 adsorption, TEM, and FTIR spectroscopy. Using the Friedel-Crafts alkylation as test reaction, the immobilized TSILs showed high efficiency and stability.

2. Experimental

2.1 Catalysts preparation

Fig. 1 shows the schematic procedures for the synthesis of immobilized HPW-PMIMPS-SBA-15 materials. N-triethoxysilylpropylimidazole(compound **1**) was synthesized by refluxing 53.00 mmol of imidazole with 50.00 mmol of 3-triethoxysilylpropylchloride in toluene (50 mL) at 70 ℃ for 24 h under a nitrogen atmosphere. 1,3-propane sulfone（10.50 mmol）was added to 2.72 g of the compound **1**, followed by stirring at 50 ℃ for 8 h under a nitrogen atmosphere. A white precipitate was filtered, washed with diethyl ether three times, and then dried in vacuum. 1-sulfonic group propyl-3-triethoxysilylpropyl-imidazolium(compound **2**) was obtained. 1.00 g of dry SBA-15 prepared according to the literature method [18] and 0.40 g of the compound **2** were dispersed in 50 mL of anhydrous toluene, and then refluxed for 24 h under nitrogen protection. After being

View Article Online
DOI: 10.1039/C4RA03531C

filtrated and washed with anhydrous ethanol, the obtained precipitate was Soxhlet extracted over ethanol for 48 h. The product was filtrated, washed with anhydrous ethanol, and dried at room temperature under vacuum overnight. The immobilized basic sulfonic -containing TSILs is designated as PMIMPS-SBA-15(compound **3**). 1.00 g of the obtained compound **3** was dispersed in 100 mL of deionized water, followed by adding various amount of 12-Tungstophosphoric Acid (HPW) according to different weight ratio of HPW to the compound **3** (n, n = 0.10, 0.20, 0.30, or 0.40), then the resultant suspension was kept stirring at room temperature for 12 h. The resulting precipitate was filtered, washed with deionized water several times, dried overnight in vacuum, and Soxhlet extracted over ethanol for 12 h. The obtained sample was denoted as xHPW-PMIMPS-SBA-15(compound **4**), where x stands for the weight ratio of HPW to the compound **3**.

For comparison purposes, the task-specific basic ionic liquid 1-(propyl-3-sulfonate) 3-methyl-imidazolium phosphotungstate ($[MIMPS]_3PW_{12}O_{40}$) was synthesized by the following procedure [19]. Methylimidazole (0.11 mol) and 1,3-propane sulfone (0.10 mol) were dissolved in toluene (20 mL) and stirred for 24 h at 50 °C under a nitrogen atmosphere. A white precipitate (MIMPS)was filtered, washed with diethyl ether three times, and then dried in vacuum. MIMPS (0.06 mol) was added to an aqueous solution of $H_3PW_{12}O_{40}$ (0.02 mol), and then the mixture was stirred at room temperature for 24 h. Water was removed in vacuum to give the product as a solid.

2.2 Catalysts Characterization

Powder X-ray diffraction (XRD) patterns were obtained with a Rigaku D/max-rC Siemens diffractometer using nickel-filtered Cu Kα as monochromatic X-ray radiation. The scattering intensities were measured over an angle range of $0.58 < 2\theta < 40$ with a step size $D(2\theta) = 0.028$ and a step time of 8 s. The nitrogen adsorption and desorption isotherms were measured at -196 ℃ on an ASAP 2020 system. Prior to the measurements, all samples were degassed under vacuum at 80℃ for 4 h. The specific surface area, A_{BET}, was determined from the linear part of the BET equation ($P/P_0 = 0.05$-0.30). The pore size distribution was derived from the adsorption branch of the N_2 isotherm using the Barrett-Joyner-Halenda (BJH) method. The total pore volume was estimated from the amount of nitrogen adsorbed at a relative pressure (P/P_0) of ca. 0.995. Pore structures of the samples were examined by TEM (Jeol, JEM-2000EXII). Fourier transformation infrared (FT-IR) spectra were obtained on a Bruker Tensor 27, scanned from 4000

View Article Online
DOI: 10.1039/C4RA03531C

cm^{-1} to 400 cm^{-1}. The sample was ground with KBr and pressed into a thin wafer.

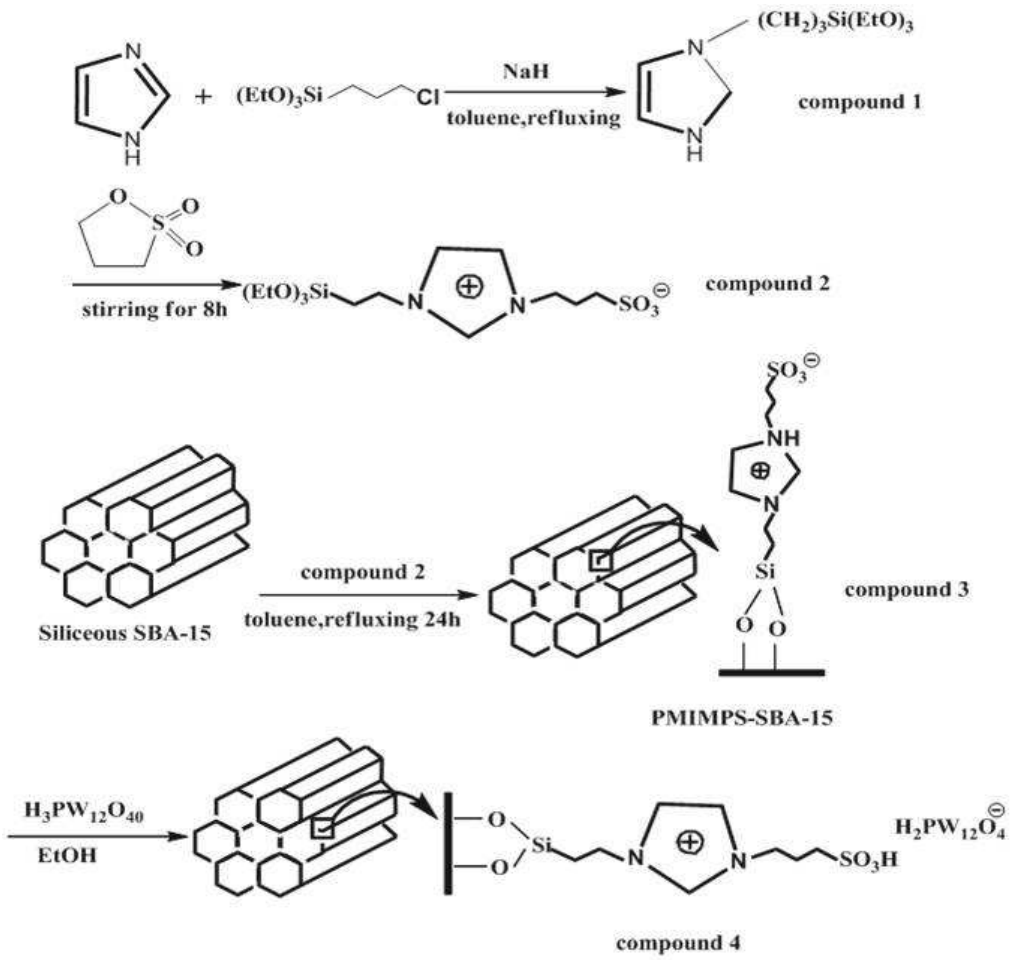

Fig. 1. Schematic procedures for the synthesis of immobilized HPW-PMIMPS-SBA-15 materials

2.3 Catalytic Tests

The alkylation reactions were carried out in a continuously stirred batch reactor under reflux conditions using a three-neck 100-ml round-bottom flask equipped with a condenser. Preliminary runs were conducted with 7.50 g (0.0721mol) of styrene, 57.35 g (0.5402 mol) of *o*-xylene (mole ratio of *o*-xylene to styrene, 7.5∶1) and 1.50 g of catalyst (20% w/w of styrene) at 120 ℃ for 180 minutes. The required amount of *o*-xylene was initially added to the reactor at the reaction temperature, followed by the desired amount of catalyst, a known amount of styrene was then added to the reaction mixture at the same temperature. After the reaction, unreacted *o*-xylene was distilled out under atmospheric pressure and then a collected part was called as crude product. The crude product was analyzed with GC-9890A gas chromatograph equipped with OV-1

View Article Online
DOI: 10.1039/C4RA03531C

capillary column and a flame ionization detector (FID). The yield of PXE was defined as follows:

$$\text{yield of PXE}(\%) = \frac{\text{actual product weight}}{\text{all theoretical product weight}} \times 100$$

$$\text{actual product weight} = \text{crude product weight} \times \text{PXE(chromatography)}\%$$

3. Results and discussion

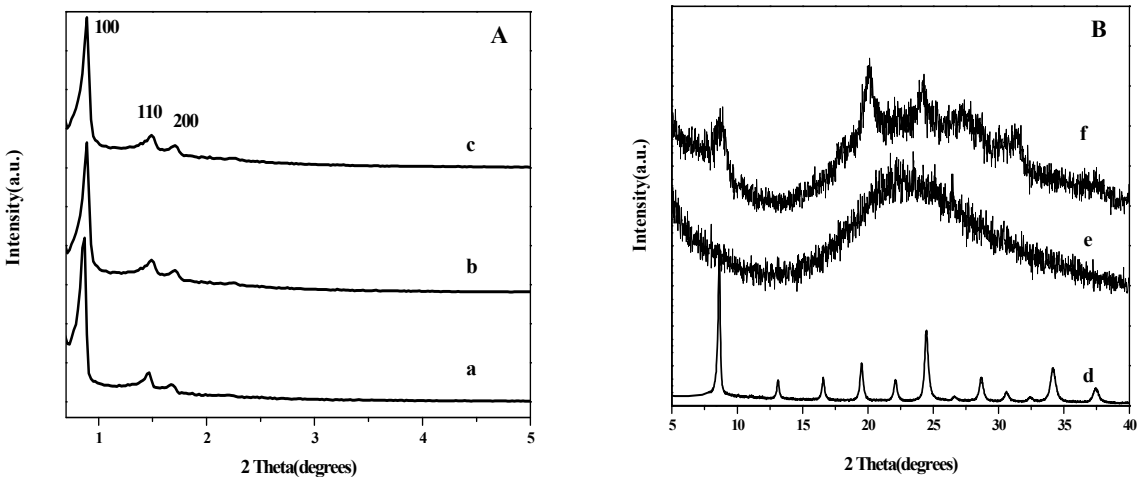

Fig. 2 Powder low-angle X-ray diffraction patterns of the samples siliceous SBA-15(A-a), PMIMPS-SBA-15(A-b) and 30%HPW-PMIMPS-SBA-15(A-c) and powder high-angle X-ray diffraction patterns of the HPW(B-d), 30%HPW-PMIMPS-SBA-15(B-e) and 40%HPW-PMIMPS-SBA-15(B-f).

The low-angle XRD patterns of the siliceous SBA-15, PMIMPS-SBA-15 and 30%HPW-PMIMPS-SBA-15, as well as the high-angle XRD patterns of the Keggin HPW, 30%HPW-PMIMPS-SBA-15 and 40%HPW-PMIMPS-SBA-15 are shown in Fig. 2. The siliceous SBA-15 showed a pattern with a very strong reflection at 2θ=0.86° for d_{100} and two other weaker reflections at 2θ=1.46° and 2θ=1.68° for d_{110} and d_{200}, respectively, associated with the quasi-regular arrangement of mesopores with hexagonal symmetry [17]. In contrast, three reflections of d_{100}, d_{110}, and d_{200} could clearly be observed for PMIMPS-SBA-15 and 30%HPW-PMIMPS-SBA-15, although the intensities of d_{100}, d_{110}, and d_{200} reflections decreased slightly and the three diffraction peaks shifted to higher angle in comparison with the siliceous SBA-15. This can be due to decreased local order, and/or the reduction of scattering contrast induced by the incorporated organic moieties and PW anions [20]. Moreover, the high-angle XRD

View Article Online
DOI: 10.1039/C4RA03531C

pattern of the 30%HPW-PMIMPS-SBA-15 does not show the distinct diffraction peaks corresponding to the crystalline HPW phase (Fig. 2B-e vs Fig. 2B-d), which suggests the high dispersion of PW in the channels of the 30%HPW-PMIMPS-SBA-15 [21]. However, at higher HPW loading(40%HPW-PMIMPS-SBA-15), the high-angle XRD pattern showed some distinct diffraction peaks corresponding to the crystalline HPW phase (Fig. 2B-f), demonstrating the agglomeration of the excessive HPW in the mesopore channels of PMIMPS-SBA-15.

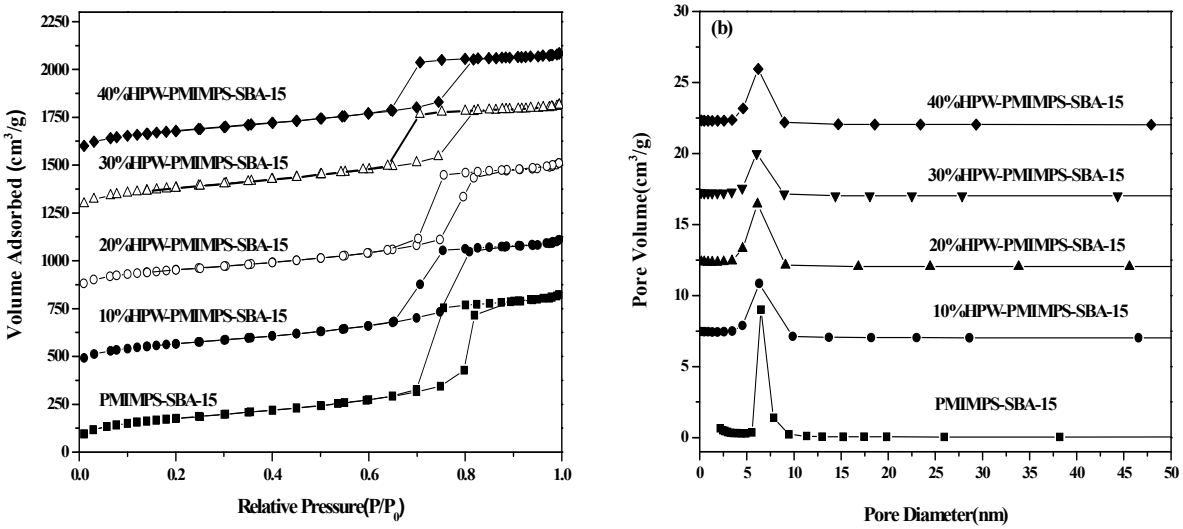

Fig. 3 Nitrogen adsorption-desorption isotherms (left) and pore size distribution (right) of the samples PMIMPS-SBA-15 and xHPW-PMIMPS-SBA-15(x=10%, 20%, 30% and 40%)

Table 1. Textural parameters of the PMIMPS-SBA-15 and xHPW-PMIMPS-SBA-15

Sample	**HPW (wt%)**	V_{total} (cm^3g^{-1})	S_{BET}[a] (m^2g^{-1})	**Pore size**[b] (nm)
PMIMPS-SBA-15	-	0.85	618	5.90
10%HPW-PMIMPS-SBA-15	10	0.70	446	5.60
20%HPW-PMIMPS-SBA-15	20	0.66	376	5.50
30%HPW-PMIMPS-SBA-15	30	0.61	363	5.48
40%HPW-PMIMPS-SBA-15	40	0.58	330	5.42

[a] BET method
[b] BJH model applied to the desorption branch of the isotherms

N_2 adsorption-desorption isotherms record the textural properties of the PMIMPS-SBA-15 and xHPW-PMIMPS-SBA-15, as shown in Fig. 3. As can be seen, all samples display typical type-IV

View Article Online
DOI: 10.1039/C4RA03531C

isotherms with a clear adsorption-desorption hysteresis loops at the relative pressure of $0.65 < P/P_0 < 0.85$ (Fig. 3 left), characteristic of mesoporous material with uniform cylindrical channel and narrow pore size distribution [17]. The shape of the isotherms varies with the ionic liquid moieties and PW anions. On the other hand, the BJH pore size distribution (calculated from the analysis of the desorption branch of the isotherms) is presented in Fig. 3 right. It can be seen that all samples exhibit a fairly uniform pore size distribution (5-7 nm). Effect of the ionic liquid moieties and PW anions loadings on the corresponding surface area, pore diameter and pore volume of HPW-PMIMPS-SBA-15 catalysts are presented in Table 1. As expected, HPW-PMIMPS-SBA-15 present decreased pore volume compared to the parent PMIMPS-SBA-15. Increased PW anions loading leads to a gradually decrease in pore volume. Especially, some pore blockage have taken place when the PW anions content increased over 40%, which suggests that the PW anions are located inside the pore indeed. These details are also reflected in the surface area and pore size of HPW-PMIMPS-SBA-15 catalysts. However, the surface area of the samples up to 30% HPW loaded was more than 300 m^2/g and the pore volume was in the range of 0.61-0.70 cm^3/g (Table 1), which is sufficient for catalytic performance.

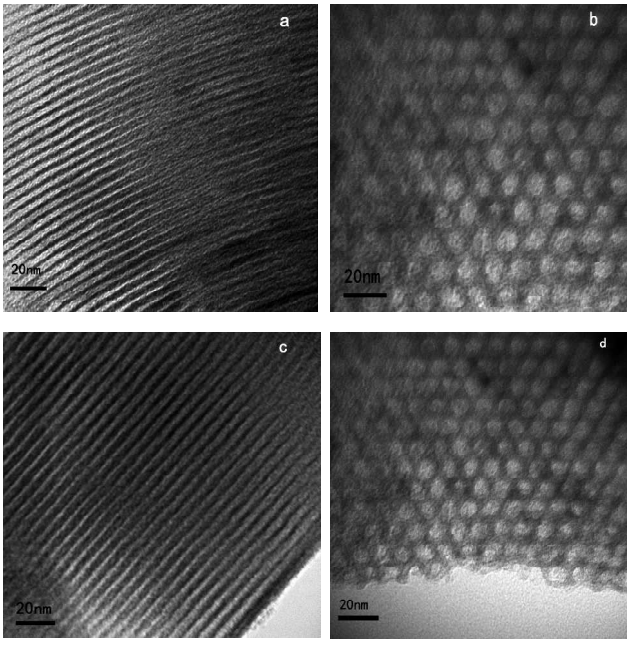

Fig. 4. Typical TEM images of PMIMPS-SBA-15 (a and b) and 30%HPW-PMIMPS-SBA-15 (c and d). The bars in the photos are 20 nm.

TEM micrographs of the representative sample PMIMPS-SBA-15 and 30%HPW-PMIMPS-SBA-15 (Fig. 4) provide a direct visualization of well-ordered hexagonal

View Article Online
DOI: 10.1039/C4RA03531C

arrays of 2D mesoporous channels particularly in the direction perpendicular to the pore axis (Fig. 4a and c) or along the direction of the pore axis (Fig. 4b and d). The TEM images confirm the intact mesostructures of all the samples even though the PW and ionic liquid moieties were loaded in the channel of SBA-15.

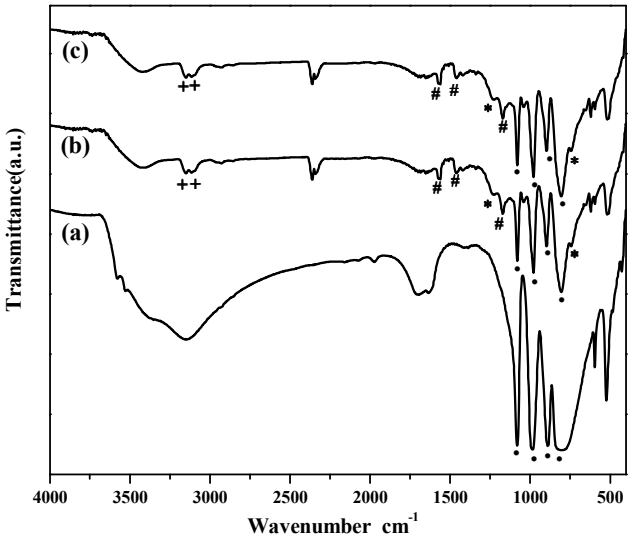

Fig. 5 FT-IR spectra of pure HPW(a), PMIMPS-SBA-15 (b) and 30%HPW-PMIMPS-SBA-15 (c)

Fig. 5 compares the FT-IR spectrum of 30%HPW-PMIMPS-SBA-15 with those of PMIMPS-SBA-15 and neat Keggin-type HPW. In the cases of the samples incorporated with the terminal HPW-based ionic complexes, 30%HPW-PMIMPS-SBA-15 represented an almost identical FT-IR spectrum to PMIMPS-SBA-15 (Fig. 5b vs. Fig. 5c). More specifically, both the samples showed vibration bands at 3160, 3118 cm^{-1} (+), 1556,1451,1170 cm^{-1} (#), and 1242,738 cm^{-1} (*), which can be assigned, respectively, to the aromatic C-H stretching in imidazolium cations, the feature vibrations of imidazolium moieties, the C-Si stretching vibrations [22]. Such observations suggest that the grafting process presented here do not change the structure of the ionic liquid. As shown in Fig. 5, four characteristic bands at around 1080, 980, 890 and 800 cm^{-1}(•) appears distinctively in the FT-IR spectrum of the Keggin-type HPW (Fig. 5a), which are assigned to asymmetric stretching vibration of P-O_a, W=O_d, W-O_b-W in corner shared octahedral and W-O_c-W in edge shared octahedral, respectively [23]. The four bands also appear in the FT-IR spectrum of the supported 30%HPW-PMIMPS-SBA-15, which indicates that the Keggin structure of PW anions is well reserved (Fig. 5c vs Fig. 5a). Therefore, combined Fig 4 and Fig 5,

View Article Online
DOI: 10.1039/C4RA03531C

it can be indicative of covalent attachment of HPW and linker with SBA-15 surface.

The catalytic activity of different catalysts is showed in Table 2. The detailed reaction scheme is shown in scheme 1, reaction (1) is the PXE formation reaction whereas reaction (2) and (3) represent the formation of styrene oligomers and more substitutes, respectively.

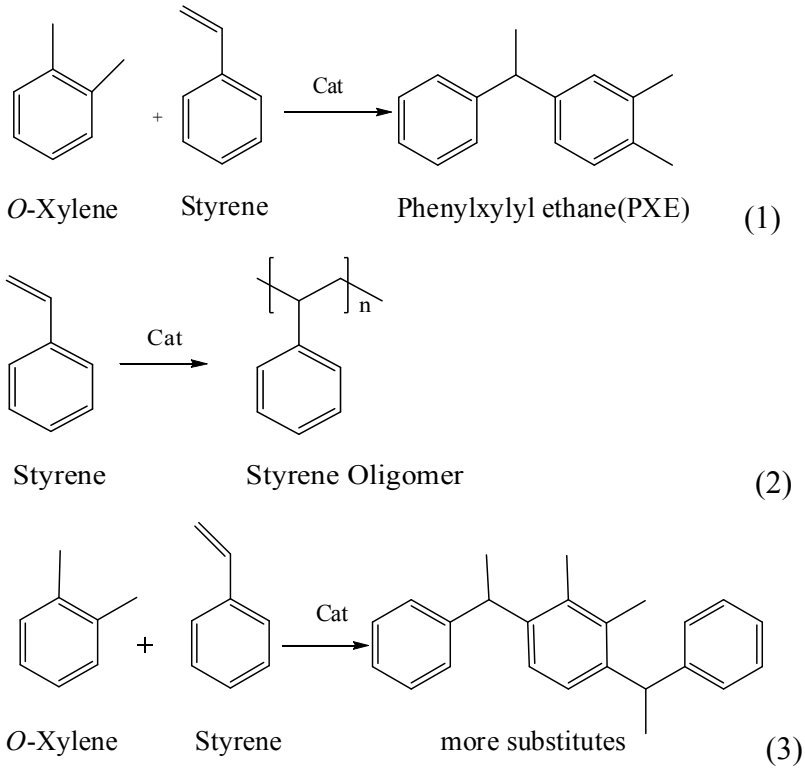

Scheme 1 Reaction scheme of alkylation of o-xylene with styrene over a heterogeneous catalyst

As shown in Table 2, the homogeneous HPW show very high catalytic performances for the reaction, however, it is difficult to separate the HPW from the product mixture. Furthermore, the SBA-15 support itself shows no activity performances. Furthermore, 30%HPW-PMIMPS-SBA-15 sample exhibits the highest product yield and good selectivity, meaning that suitable concentration of PW anions is advantageous to the reaction. In this case a significant difference is found among these catalysts as a function of loading the PW anions. The PXE yield decreases in the following order: 30%HPW-PMIMPS-SBA-15 (93.9%) > 40%HPW-PMIMPS-SBA-15 (91.2%) > 20%HPW-PMIMPS-SBA-15 (80.5%) > 10%HPW-PMIMPS-SBA-15 (71.8%). In the case of 40%HPW-PMIMPS-SBA-15 the product yield is found to be less compared to 30%HPW-PMIMPS-SBA-15 catalyst, which is probably due to the blocking of active sites by the dense Keggin structure, thereby changing the

View Article Online
DOI: 10.1039/C4RA03531C

morphology of the support (mesopore diameter and volume) and giving diffusional constraints. In addition, it is worth of noting that the $[MIMPS]_3PW_{12}O_4$ shows good catalytic performances, because it has sufficient PW anions content.

Table 2. Activity of various catalysts in alkylation of *o*-xylene with styrene [a]

catalyst	Styrene conversion (%)	PXE Yield [c] (%)	PXE Selectivity [d] (%)
SBA-15	-	-	-
HPW [b]	100	97.9	9:1
10%HPW-PMIMPS-SBA-15	74.8	71.8	9:1
20%HPW-PMIMPS-SBA-15	83.9	80.5	9:1
30%HPW-PMIMPS-SBA-15	97.8	93.9	9:1
40%HPW-PMIMPS-SBA-15	95.0	91.2	9:1
$[MIMPS]_3PW_{12}O_4$	94.5	90.8	9:1

[a] Reaction conditions: *o*-xylene： styrene = 7.5∶1,reaction temperature=120℃, reaction time= 3.0h, catalyst loading =20% (w/w of styrene).
[b] Hompgeneous catalyst, 0.30g.
[c] Isolated yield based on the amount of styrene.
[d] Ratio of para-to-ortho product.

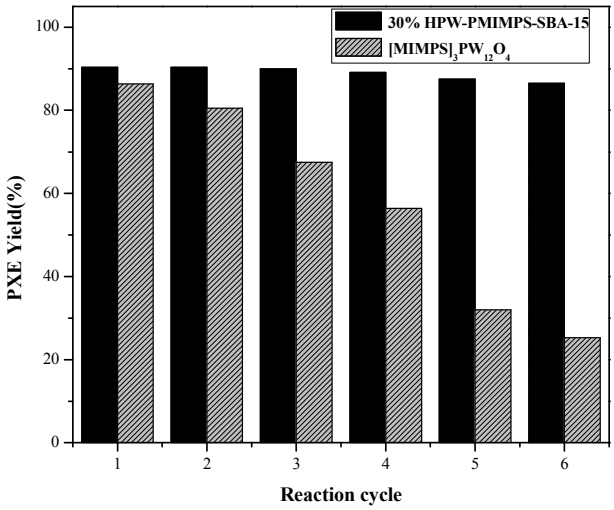

Fig. 6 Catalytic Stability of the 30%HPW-PMIMPS-SBA-15 and $[MIMPS]_3PW_{12}O_4$ catalysts in the alkylation of *o*-xylene with styrene(Reaction conditions: *o*-xylene ：styrene = 7.5∶1, reaction temperature=120℃, reaction time= 3.0h, catalyst loading =20% (w/w of styrene).

Stability and reusability of the catalyst were very important for any catalytic system. The

View Article Online
DOI: 10.1039/C4RA03531C

catalytic reusability of the 30%HPW-PMIMPS-SBA-15 and $[MIMPS]_3PW_{12}O_4$ catalysts was evaluated by carrying out the reaction with used catalyst under the optimized conditions. After completion of the reaction, the catalyst was easily recovered from the reaction mixture by centrifugation and, used for the subsequent catalytic runs without further activation. The data obtained are shown in Fig. 6. Interestingly, the activity decreased slightly after reuse of the 30%HPW-PMIMPS-SBA-15 for six times. Indeed, the yield of PXE product was as high as 89.5% even after the 30%HPW-PMIMPS-SBA-15 was recycled for six times. On contrast, the yield of PXE product significantly decreased from 90.8 to 30.3% as pure ionic liquid of $[MIMPS]_3PW_{12}O_4$ was recycled for six times under the same reaction conditions. These results indicate that the immobilized heteropolyanion-based ionic liquid presented here possesses much higher catalytic efficiency in comparison with the corresponding pure ionic liquid. Therefore, immobilized ionic liquid catalyst on porous carriers used as heterogeneous catalysts can overcome the mass transfer problems in practical application. Indeed, through immobilized ionic liquid catalyst on various supports can obtain larger specific surface area and more stable. And after reaction, it can be also easier separation and better reusability.

4. Conclusions

In summary, the work herein presented fabricating HPW-based ionic liquid immobilized on mesoporous silica SBA-15 by totally anion-exchange. The resultant catalysts showed better catalytic efficiency and reusability than the corresponding task-specific basic ionic liquid in the alkylation of *o*-xylene with styrene. It was found that the occasion of adding HPW during the synthesis of catalysts played a crucial role in PW anions loading and successive catalytic performance. Moreover, the use of such heterogeneous catalyst can decrease the consumption of ionic liquid remarkably. As such, the synthesis procedure can be simplified significantly, which may open an opportunity for wide applications of immobilized heteropolyanion-based ionic liquid in catalysis.

Acknowledgments

The authors are grateful to the financial supports of National Natural Science Foundation of China (Grant No. 21306023, 21376051, 21106017), Natural Science Foundation of Jiangsu

View Article Online
DOI: 10.1039/C4RA03531C

Province of China (Grant No. BK20131288), Fund Project for Transformation of Scientific and Technological Achievements of Jiangsu Province of China (Grant No. BA2011086), Key Program for the Scientific Research Guiding Found of Basic Scientific Research Operation Expenditure of Southeast University (Grant No. 3207043101) and Instrumental Analysis Fund of Southeast University.

Refenrences

1. A. B. Dixit and G. D. Yadav, *React. Funct. Polym.*, 1996, **31**, 251-263.
2. B. S. Kwak and T. J. Kim, *Catal. Lett.*, 1999, **59**, 55-60.
3. A. Sato, I. Shimizu, G. Mesalito, US 4289918A[P], 1981-09-15
4. J. H. Lunsford, H. Sang, S. M. Campbell, C. H. Liang and R. G. Anthony, *Catal. Lett.*, 1994, **27**, 305-314.
5. Y. P. Wang, R. J. Qu, C.H. Wang, *Appl. Chem. Ind.* , 2009, **36**, 822-826.
6. F. E. Celik, H. Lawrence and A. T. Bell, *J. Mol. Catal. A-Chem.*, 2008, **288**, 87-96.
7. X. L. Sheng, Y. M. Zhou, Y. W. Zhang, M. W. Xue and Y. Z. Duan, *Chem. Eng. J.*, 2012, **179**, 295-301.
8. X. L. Sheng, Y. M. Zhou, Y. W. Zhang, Y. Z. Duan and M. W. Xue, *Catal. Lett.*, 2012, **142**, 360-367.
9. D. R. MacFarlane, J. M. Pringle, K. M. Johansson, S. A. Forsyth and M. Forsyth, *Chem. Commun.*, 2006, 1905-1917.
10. H. Li, P. S. Bhadury, B. A. Song and S. Yang, *RSC Adv.*, 2012, **2**, 12525-12551.
11. J. M. Miao, H. Wan and G. F. Guan, *Catal. Commun.*, 2011, **12**, 353-356.
12. F. J. Liu, S. F. Zuo, W. P. Kong and C. Z. Qi, *Green Chem.*, 2012, **14**, 1342-1349.
13. H. H. Zhao, H. L. Song and L. J. Chou, *Microporous Mesoporous Mat.*, 2013, **181**, 182-191.
14. H. H. Zhao, N. Y. Yu, J. Q. Wang, D. Y. Zhuang, Y. Ding, R. Tan and D. H. Yin, *Microporous Mesoporous Mat.*, 2009, **122**, 240-246.
15. C. DeCastro, E. Sauvage, M. H. Valkenberg and W. F. Holderich, *J. Catal.*, 2000, **196**, 86-94.
16. G. J. Wang, N. Y. Yu, L. Peng, R. Tan, H. H. Zhao, D. H. Yin, H. Y. Qiu, Z. H. Fu and D. L. Yin, *Catal. Lett.*, 2008, **123**, 252-258.
17. J. M. Miao, H. Wan, Y. B. Shao, G. F. Guan and B. Xu, *J. Mol. Catal. A-Chem.*, 2011, **348**, 77-82.
18. D. Y. Zhao, J. L. Feng, Q. S. Huo, N. Melosh, G. H. Fredrickson, B. F. Chmelka and G. D. Stucky, *Science*, 1998, **279**, 548-552.
19. Y. Leng, J. Wang, D. R. Zhu, X. Q. Ren, H. Q. Ge and L. Shen, *Angew. Chem.-Int. Edit.*, 2009, **48**, 168-171.
20. S. Jana, B. Dutta, R. Bera and S. Koner, *Langmuir*, 2007, **23**, 2492-2496.
21. G. Karthikeyan and A. Pandurangan, *J. Mol. Catal. A-Chem.*, 2009, **311**, 36-45.
22. A. Bordoloi, S. Sahoo, F. Lefebvre and S. B. Halligudi, *J. Catal.*, 2008, **259**, 232-239.
23. T. Nakashima and N. Kimizuka, *J. Am. Chem. Soc.*, 2003, **125**, 6386-6387.